

# Photons and Exclusive Processes at Hadron Colliders

*Joakim Nystrand*

Department of Physics and Technology, University of Bergen, Bergen, Norway

DOI: <http://dx.doi.org/10.3204/DESY-PROC-2009-03/Nystrand>

The theoretical and experimental aspects of particle production from the strong equivalent photon fluxes present at high energy hadron colliders are reviewed. The goal is to show how photons at hadron colliders can improve what we have learnt from experiments with lepton beams. Experiments during the last 5-10 years have shown the feasibility of studying photoproduction in proton-proton and heavy-ion collisions. The experimental and theoretical development has revealed new opportunities as well as challenges.

## 1 Introduction

During the last decade the idea to study electromagnetic particle production at hadron and heavy-ion colliders has developed theoretically as well as experimentally. At the previous conference in this series (Photon 07, held at the Sorbonne in Paris), a session was devoted to this topic. I gave a summary of photoproduction at hadron colliders, in particular in heavy-ion collisions, at that meeting [1]. Since then, several new results have been published and an update of the latest developments will be given here. More comprehensive reviews of the field can be found e.g. in [2] and [3].

There are several reasons to study photon-induced reactions in collisions between hadrons. At the Large Hadron Collider (LHC) at CERN, the accessible two-photon center-of-mass energies will be much higher than at LEP and the photon-nucleon energies will be higher than at HERA. The LHC will thus explore a new and uncharted territory also in interactions mediated by photons. Heavy-ion interactions at the Relativistic Heavy-Ion Collider and at the LHC provide an opportunity to study photons from strong electromagnetic fields where the coupling is  $Z\sqrt{\alpha}$  rather than  $\sqrt{\alpha}$ . At a hadron collider both projectiles can act as photon emitter and target, and this leads to some interesting interference phenomena, which will be discussed below. Furthermore, the electromagnetic contribution is important for understanding other types of exclusive particle production, e.g. through Pomeron+Pomeron interactions in  $pp$  or  $p\bar{p}$  collisions. It has been proposed to use two-photon production of  $\mu^+\mu^-$ -pairs as a luminosity monitor at the LHC.

To separate the electromagnetic interactions from the “background” of strong, hadronic processes, it is in practice necessary to restrict the study to so-called ultra-peripheral collisions, where the impact parameters are larger than the sum of the beam particle radii. This means impact parameters in the range  $\approx 1.4(14) - 100$  fm in proton-proton (heavy-ion) collisions. The upper range 100 fm is somewhat arbitrary but in practice the fields at current colliders are too weak to produce particles outside this range. The exception is production of

low-mass  $e^+e^-$ -pairs, where impact parameters above 1000 fm can give a significant contribution. Experimentally, interactions mediated by photons can be separated from purely hadronic interactions by their lower multiplicity and the presence of rapidity gaps. If the entire event is reconstructed, charge conservation and the low total transverse momentum also provide strong background rejection.

## 2 Results from RHIC

Ultra-peripheral collisions have been studied at the Relativistic Heavy-Ion Collider (RHIC) at Brookhaven National Laboratory by the two large experiments PHENIX and STAR. The first results on  $\rho^0$  photoproduction were published by the STAR collaboration based on data from the first run at RHIC in the year 2000. STAR has so far mainly focussed on low-mass states, such as photoproduction of the  $\rho^0$  meson and low-mass  $e^+e^-$  pairs. The study of ultra-peripheral collisions in PHENIX has been directed towards heavy vector meson production ( $J/\Psi$ ) and high-mass  $e^+e^-$  pairs. The first preliminary results from PHENIX were presented at the Quark Matter 2005 conference [4], and earlier this year the final results were published [5]. The final results also include cross sections for two-photon production of  $e^+e^-$  pairs.

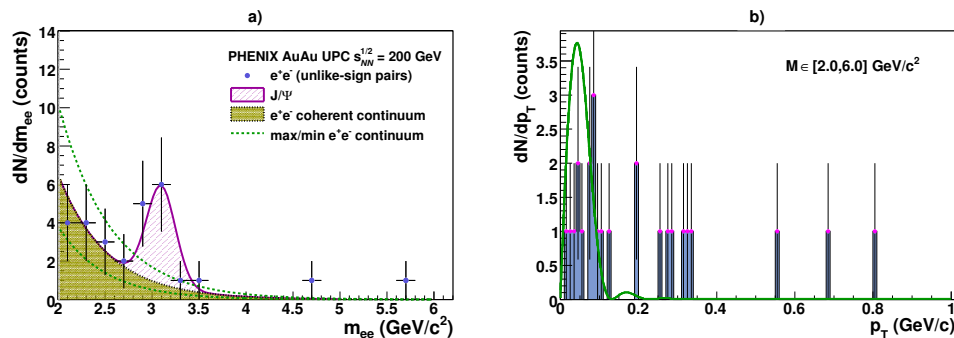


Figure 1: Invariant mass (a) and transverse momentum (b) distributions of  $e^+e^-$  pairs in ultra-peripheral Au+Au collisions as measured by PHENIX[5]. The event selection is described in the text.

PHENIX has implemented a trigger where an energy deposit of  $E \gtrsim 0.8$  GeV in the mid-rapidity electromagnetic calorimeters is combined with two rapidity gaps at intermediate rapidities. The rapidity gaps are defined by an absence of a signal in the Cherenkov Beam-Beam Counters (BBC) covering the pseudorapidity range  $3.0 < |\eta| < 3.9$  on either side of midrapidity. It is furthermore required that there should be a signal ( $E \gtrsim 30$  GeV) in one or both of the Zero-Degree Calorimeters (ZDC) situated 18 m downstream from the interaction point. This requirement means that the central production occurs in coincidence with exchange of one or more additional photons which lead to the break up of one or both nuclei.

A data sample with an integrated luminosity of  $141 \pm 12 \mu\text{b}$  from the 2004 high-luminosity run at RHIC has been analyzed. This luminosity corresponds to around  $960 \cdot 10^6$  inelastic Au+Au events ( $\sigma_{inel} = 6.8$  b). The UPC trigger as described above collected  $8.5 \cdot 10^6$  events out of which  $6.7 \cdot 10^6$  satisfied standard data quality assurance criteria. The electrons and positrons were tracked and identified in the PHENIX central tracking arms, covering  $|\eta| <$

$m_{inv}$ [GeV]	$d\sigma/dm_{inv}dy$ ( $ y  < 0.35$ )	$d\sigma/dm_{inv}dy$ ( $ y  < 0.35,  \eta_{1,2}  < 0.35$ )
$2.0 \leq m_{inv} \leq 2.8$	$86 \pm 23(stat) \pm 16(syst)$	$0.95 \pm 0.25(stat) \pm 0.18(syst)$
$2.0 \leq m_{inv} \leq 2.3$	$129 \pm 47(stat) \pm 28(syst)$	$1.43 \pm 0.52(stat) \pm 0.31(syst)$
$2.3 \leq m_{inv} \leq 2.8$	$60 \pm 24(stat) \pm 14(syst)$	$0.65 \pm 0.26(stat) \pm 0.15(syst)$

Table 1: Differential cross sections for two-photon production of  $e^+e^-$  pairs [5]. The variables  $y$  and  $m_{inv}$  refer, respectively, to the rapidity and invariant mass of the pair. The rightmost column shows the cross section when one requires both the  $e^+$  and  $e^-$  to be within  $|\eta| < 0.35$ .

0.35 and  $\Delta\phi = 90^\circ$  each. Tracking was performed by multi-layer drift chambers and multi-wire proportional chambers in each arm, and electrons were identified by their signals in the Ring-Imaging-Cherenkov (RICH) detectors and the electromagnetic calorimeters. In the offline analysis, it was required that the event should contain exactly 2 tracks of opposite charge satisfying the UPC electron/positron identification criteria and that the event vertex should be within  $|Z| < 30$  cm from the center of the detector. It was required that each electron/positron should have  $E > 1$  GeV to be well above the trigger threshold ( $E \gtrsim 0.8$  GeV). This gave a sample with 28 events, the invariant mass and  $p_T$  distributions of which are shown in Fig. 1. There was no like-sign background after the offline cuts had been applied. The results are consistent with production of  $e^+e^-$ -pairs through two-photon interactions,  $\gamma + \gamma \rightarrow e^+e^-$ , and photonuclear production (coherent and incoherent) of  $J/\Psi$ ,  $\gamma + Au \rightarrow J/\Psi + Au$ , followed by the decay  $J/\Psi \rightarrow e^+e^-$ . The background from hadronically produced  $e^+e^-$  pairs in the ultra-peripheral sample was estimated from measurements of  $e^+e^-$  pairs in proton-proton collisions and was found to be negligible ( $< 1$  event). The majority of the events are from coherent production, as can be seen from the transverse momentum distribution in Fig. 1 b). The curve shows for comparison the nuclear (Au) form factor.

The cross section for  $J/\Psi$  production,  $d\sigma/dy = 76 \pm 31(stat) \pm 15(syst)\mu\text{b}$  with nuclear break up, is consistent with theoretical predictions [6, 7, 8, 9], but the size of the experimental errors precludes a discrimination between the models. The cross sections for continuum  $e^+e^-$  production are shown in Table 1. The results are in good agreement with calculations using the method of equivalent photons as implemented in the Starlight Monte Carlo [11].

The mid-rapidity cross section for  $J/\Psi$  is a measure of the  $J/\Psi$ + Nucleon cross section in nuclear matter [7] and is also affected by nuclear gluon shadowing [10]. Recent calculations by Baltz [12] for two-photon production of di-muons and di-electrons have found that higher-order terms reduce the cross section by 20-30% in heavy-ion collisions. A recent calculation has however not found such large reductions from higher order terms, particularly not for  $\mu^+\mu^-$  pairs [13]. A measurement with smaller errors could settle this issue experimentally.

The STAR collaboration has studied coherent and incoherent photoproduction of  $\rho^0$  mesons in Au+Au collisions at  $\sqrt{s_{NN}} = 130$  and 200 GeV [14, 15]. The pions from the decay  $\rho^0 \rightarrow \pi^+\pi^-$  were reconstructed in the STAR Time-Projection Chamber (TPC), which covers the pseudorapidity range  $|\eta| < 1$  with full coverage in azimuth. Two trigger classes were defined. One class was based on having two roughly back-to-back hits in the Central Trigger Barrel (CTB), a set of 240 scintillators surrounding the TPC. This trigger (“topology trigger”) selects photoproduced  $\rho^0$  mesons with and without nuclear break up. The second trigger class (“minimum bias (MB)”) required the events to have a signal in both ZDCs, and thus selected photoproduction

in coincidence with mutual Coulomb breakup of both Au nuclei. The cross sections, rapidity and  $p_T$  distributions have been published earlier and have been found to be in good agreement with calculations [14, 15].

Both nuclei can act as photon emitter and target in an ultra-peripheral collision. Since the two possibilities cannot be distinguished, they might interfere quantum mechanically. The separation of the two nuclei when a  $\rho^0$  meson is produced at RHIC energies is typically 14–40 fm, with a different distribution depending on whether the  $\rho^0$  is produced with or without nuclear breakup. The median impact parameters are  $\langle b \rangle = 46$  fm for the total production and  $\langle b \rangle = 18$  fm with mutual break up [6]. The  $\rho^0$  meson is always produced near the surface of one of the nuclei because of the short range of the nuclear force. The system thus acts as a two-source interferometer and, depending on the separation of the nuclei and the wave length of the  $\rho^0$ , interference might occur. The interference will be destructive in collisions between particles and constructive in collisions between particles and anti-particles. For production at mid-rapidity, where the amplitudes for the two possibilities are equal, the cross section for a meson with transverse momentum  $p_T$  in a collision with impact parameter  $\vec{b}$  is

$$\sigma(p_T, \vec{b}) = 2\sigma_1(p_T, \vec{b}) \left( 1 \pm \cos(p_T \cdot \vec{b}) \right), \quad (1)$$

where  $\sigma_1(p_T, \vec{b})$  is the cross section for emission from a single source. The total production cross section is obtained by integrating over all allowed impact parameters. For  $p_T \ll 1/\langle b \rangle$ , the cross section will be affected by the interference. This is illustrated in Fig. 2, where the solid curve shows the expected  $t = p_T^2$  spectrum with interference and the dashed curve shows the expected spectrum without interference. The smaller mean impact parameters in collisions with nuclear breakup means that the interference extends to higher transverse momenta, as seen in Fig. 2b.

The presence of interference and its effect on the vector meson transverse momentum spectrum was predicted [16]. It has now been experimentally confirmed by the STAR collaboration [17]. The measured transverse momentum distributions for the two trigger classes are shown in Fig. 3. As one moves away from mid-rapidity, the amplitudes for the two target and photon-emitter configurations will be different and one expects the interference to decrease. This can be seen in the two plots to the right in Fig. 3.

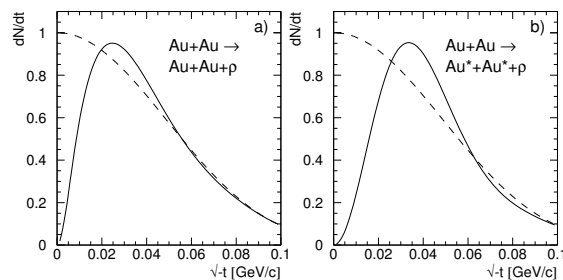


Figure 2: Predicted  $\rho^0$  transverse momentum spectra with (solid curve) and without (dashed curve) interference [6, 16]. The left plot shows the spectrum for all events while the right plot shows the spectrum for events with mutual Coulomb break up.

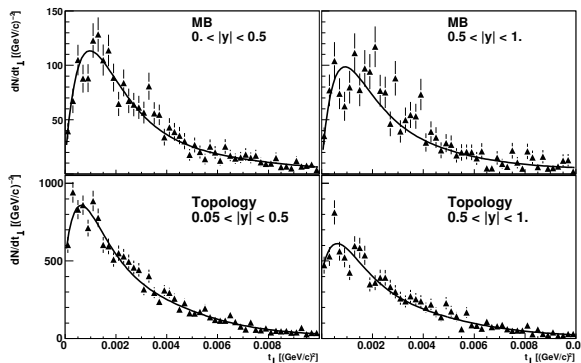


Figure 3: Transverse momentum ( $p_T^2 = t_\perp$ ) spectrum for photoproduction of  $\rho^0$  mesons in ultra-peripheral Au+Au collisions as measured by STAR [17]. The top plots are for minimum bias data and the bottom plots are for the topology trigger. The plots in the left column show production at mid-rapidity and those in the right column show production away from mid-rapidity. The curves are fits to a function with an interference term.

What makes this interference particularly interesting is the fact that the life-time of the  $\rho^0$  is much smaller than the separation between the nuclei divided by the speed of light. The interference must therefore occur between the decay products of the  $\rho^0$ , which are in an entangled state. The interference is the result of the large separation between the nuclei in an ultra-peripheral collision and is expected to be different for other coherent production mechanisms, e.g. Odderon–Pomeron fusion.

### 3 Results from the Tevatron

Two-photon and photonuclear interactions have been studied by the CDF collaboration in proton-anti-proton collisions at the Tevatron. The latest results include exclusive di-muon production in the invariant mass range  $3 \leq m_{\mu\mu} \leq 4$  GeV [18] and two-photon production of di-leptons with  $m_{ll} > 40$  GeV [19]. The produced particles have been detected at central rapidities,  $|\eta| < 0.6$  for intermediate mass di-muons and  $|\eta| < 4$  for the high mass di-leptons. The centrally produced particles are observed in an otherwise empty event, which is defined by other detectors with a coverage out to  $|\eta| < 7.4$ . Further details on the experimental setup, trigger, and the exact phase space coverage can be found in Refs. [18, 19].

The exclusive di-muon events were identified as coming from exclusive photoproduction of  $J/\Psi$  and  $\Psi'$  followed by the decay to  $\mu^+\mu^-$  and two-photon continuum production of  $\mu^+\mu^-$  pairs. The background from the  $\chi_c$  mesons produced in exclusive Pomeron-Pomeron interactions decaying to  $\chi_c \rightarrow J/\Psi + \gamma$  was estimated. Measurements were made where a  $J/\Psi$  was produced in coincidence with a photon with energy  $E_\gamma > 80$  MeV. From this, it could be estimated that the background from  $\chi_c$  events where the photon is not detected contributed about 4% to the exclusive  $J/\Psi$  sample.

The exclusive events can be simulated with the Starlight Monte Carlo, which is based on the model in [25]. The photon-proton cross sections as measured by experiments at HERA and at fixed target experiments with lepton beams are used as input to the calculations. These are

combined with the equivalent photon spectrum to give the cross section for  $p + \bar{p} \rightarrow p + \bar{p} + V$ , where  $V$  is a vector meson. Starlight can also calculate the cross section for  $\mu^+\mu^-$  pairs produced in two-photon interactions. The differential cross section,  $d\sigma/dy$ , for vector meson production is given by

$$\frac{d\sigma(p+\bar{p}\rightarrow p+\bar{p}+V)}{dy} = k_1 \frac{dn_\gamma}{dk_1} \sigma_{\gamma p}(k_1) + k_2 \frac{dn_\gamma}{dk_2} \sigma_{\gamma p}(k_2). \quad (2)$$

Here,  $dn/dk$  is the photon spectrum and  $\sigma_{\gamma p}$  the cross section for  $\gamma + p \rightarrow V + p$ . A  $J/\Psi$  produced at central rapidity within  $|y| < 0.5$  corresponds to photoproduction with photon-proton center-of-mass energies between  $60 \leq W_{\gamma p} \leq 100$  GeV. Exclusive  $J/\Psi$  and  $\Psi'$  production has been studied at HERA in this energy range by both the Zeus [20] and H1 [21] collaborations. The  $\gamma + p \rightarrow J/\Psi + p$  cross sections are thus known experimentally, with errors typically in the range 6–9 %.

The photon spectrum associated with a relativistic proton can be calculated from that of a point charge modulated by a form factor [22]. A problem with this approach is that it does not properly exclude collisions where the protons interact hadronically. A different approach is therefore used here. The method is similar to that used for nuclear collisions, where one has to require that the impact parameter be larger than the sum of the nuclear radii to exclude strong interactions [23]. The proton has a more diffuse surface, however, so applying a sharp cut-off in impact parameter space is unphysical. A more realistic approach is to calculate the (hadronic) interaction probability as function of impact parameter by applying a Fourier transform to the  $pp$  elastic scattering amplitude [24]. To set a conservative upper limit on the photon spectrum, it is also calculated with a cut on the impact parameter  $b > 0.7$  fm. This gives a photon spectrum very similar to that obtained when using the proton form factor.

The transverse momentum distributions for the three final states are shown in Fig. 4 together with Starlight predictions. The transverse momenta of the vector mesons reflect the proton form factor and extend out to around  $\approx 1$  GeV/c, whereas the transverse momenta of the two-photon final state are considerably lower. The agreement between data and Starlight is very good.

For the calculations of the cross sections, the latest results from HERA were used to make a new fit to the  $\gamma + p \rightarrow V + p$  cross sections. These fits are slightly different from the ones used earlier [25]. The uncertainties in the calculated cross sections are determined from the uncertainty in the measured  $\gamma p$  cross sections and the calculation of the photon spectrum with

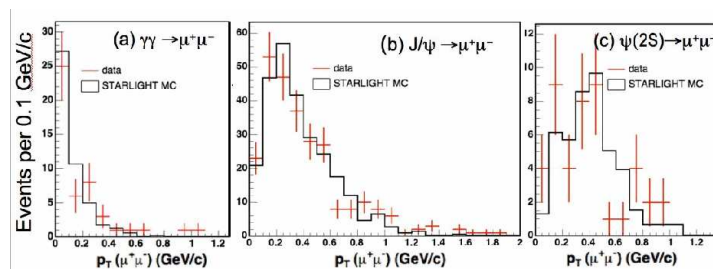


Figure 4: Transverse momentum distributions of exclusive  $\mu^+\mu^-$  pairs in  $p\bar{p}$  collisions, as measured by the CDF collaboration [18]. The crosses show the experimental results and the histograms are the Starlight predictions, normalized to the data. Fig. a) shows  $\mu^+\mu^-$  pairs in the invariant mass ranges  $3.2 \leq m_{inv} \leq 3.6$  and  $3.8 \leq m_{inv} \leq 4.0$  GeV.

$b > 0.7$  fm. The results are

$$J/\Psi : \left. \frac{d\sigma}{dy} \right|_{y=0} = 2.7^{+0.6}_{-0.2} \text{ nb} \quad , \quad \Psi' : \left. \frac{d\sigma}{dy} \right|_{y=0} = 0.45^{+0.11}_{-0.04} \text{ nb} . \quad (3)$$

These can be compared with the measured values,  $3.92 \pm 0.25(stat) \pm 0.52(syst)$  nb and  $0.53 \pm 0.09(stat) \pm 0.01(syst)$  nb, for the  $J/\Psi$  and  $\Psi'$ , respectively [18]. The measured cross section for the  $J/\Psi$  is thus about two standard deviations above the calculated value and about one standard deviation above the calculated upper limit. The CDF collaboration has concluded that the upper limit for an Odderon contribution (Odderon+Pomeron  $\rightarrow J/\Psi$ ) is less than  $d\sigma(y=0)/dy < 2.3$  nb with 95% confidence level.

## 4 Outlook to the LHC

The results from RHIC and the Tevatron show the feasibility of studying two-photon and photon-nucleon interactions at hadron colliders. The results have been found to be in general agreement with predictions, but the statistics at least for heavy final states have so far been rather low.

The situation should be more advantageous at the LHC for at least two reasons: First, the cross section increases dramatically with the increased collision energy. This is illustrated in Fig. 5, which shows the excitation function for  $J/\Psi$  production at mid-rapidity in heavy-ion collisions. The increase in cross section is about a factor of 100 between RHIC and LHC energies. Secondly, the large and versatile experiments at the LHC should have the capability to trigger on and reconstruct particles produced in ultra-peripheral collisions over a wide range of phase space.

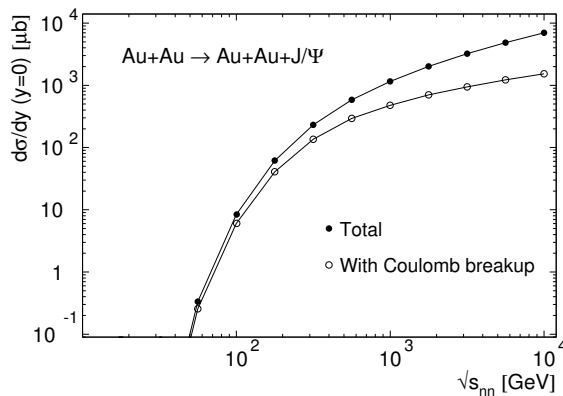


Figure 5: Calculated excitation function for mid-rapidity photoproduction of  $J/\Psi$  in Au+Au collisions, based on [6].

Several topics can be studied in ultra-peripheral collisions at the LHC. The CMS collaboration has for example investigated the possibilities for studying exclusive  $\Upsilon$  production in Pb+Pb collisions [26] and two-photon production of supersymmetric pairs in pp collisions [27].

ALICE, which is primarily aimed for studying heavy-ion collisions, has performed simulations of  $J/\Psi$  and two-photon production in heavy-ion and proton-proton collisions [28].

Most studies so far, both at the existing colliders RHIC and the Tevatron as well as at the LHC, have focussed on exclusive production of a single particle or pair of particles. It should however be possible to extract as much information from inclusive processes, for example heavy quark production from photon-gluon fusion and photon-induced jet production.

To summarize, ultra-peripheral collisions are an interesting enhancement of the physics programs at hadron colliders. They can be studied at existing and planned experiments with no or only minor modifications. The results from RHIC and the Tevatron have followed the theoretical expectations. Further studies at the LHC and at existing accelerators with increased luminosities will hopefully lead to useful constraints on e.g. the parton density distributions and possibly even to the discovery of new phenomena.

## References

- [1] J. Nystrand, Nucl. Phys. Proc. Suppl. **184** (2008) 146.
- [2] C. A. Bertulani, S. R. Klein and J. Nystrand, Ann. Rev. Nucl. Part. Sci. **55** (2005) 271.
- [3] K. Hencken *et al.*, Phys. Rept. **458** (2008) 1.
- [4] D. G. d'Enterria, arXiv:nucl-ex/0601001.
- [5] S. Afanasiev *et al.* [PHENIX Collaboration], Phys. Lett. B **679** (2009) 321.
- [6] S. Klein and J. Nystrand, Phys. Rev. C **60** (1999) 014903; A. J. Baltz, S. R. Klein and J. Nystrand, Phys. Rev. Lett. **89** (2002) 012301.
- [7] M. Strikman, M. Tverskoy and M. Zhalov, Phys. Lett. B **626** (2005) 72
- [8] Yu. P. Ivanov, B. Z. Kopeliovich and I. Schmidt, arXiv:0706.1532 [hep-ph].
- [9] V. P. Goncalves and M. V. T. Machado, J. Phys. G **32** (2006) 295; V. P. Goncalves and M. V. T. Machado, arXiv:0706.2810 [hep-ph].
- [10] A. L. Ayala Filho, V. P. Goncalves and M. T. Griep, Phys. Rev. C **78** (2008) 044904.
- [11] A. J. Baltz, Y. Gorbunov, S. R. Klein and J. Nystrand, Phys. Rev. C **80** (2009) 044902.
- [12] A. J. Baltz, Phys. Rev. Lett. **100** (2008) 062302; Phys. Rev. C **80** (2009) 034901.
- [13] U. D. Jentschura and V. G. Serbo, arXiv:0908.3853 [hep-ph], to appear in Eur. Phys. J. C.
- [14] C. Adler *et al.* [STAR Collaboration], Phys. Rev. Lett. **89** (2002) 272302.
- [15] B. I. Abelev *et al.* [STAR Collaboration], Phys. Rev. C **77** (2008) 034910.
- [16] S. R. Klein and J. Nystrand, Phys. Rev. Lett. **84** (2000) 2330.
- [17] B. I. Abelev *et al.* [STAR Collaboration], Phys. Rev. Lett. **102** (2009) 112301.
- [18] T. Aaltonen *et al.* [CDF Collaboration], Phys. Rev. Lett. **102** (2009) 242001 [arXiv:0902.1271 [hep-ex]].
- [19] T. Aaltonen *et al.* [CDF Collaboration], Phys. Rev. Lett. **102** (2009) 222002.
- [20] S. Chekanov *et al.* [ZEUS Collaboration], Eur. Phys. J. C **24** (2002) 345.
- [21] A. Aktas *et al.* [H1 Collaboration], Eur. Phys. J. C **46** (2006) 585.
- [22] M. Drees and D. Zeppenfeld, Phys. Rev. D **39** (1989) 2536.
- [23] R. N. Cahn and J. D. Jackson, Phys. Rev. D **42** (1990) 3690; G. Baur and L. G. Ferreira Filho, Nucl. Phys. A **518** (1990) 786.
- [24] L. Frankfurt, C. E. Hyde, M. Strikman and C. Weiss, Phys. Rev. D **75** (2007) 054009.
- [25] S. R. Klein and J. Nystrand, Phys. Rev. Lett. **92** (2004) 142003.
- [26] D. G. d'Enterria *et al.* [CMS Collaboration], J. Phys. G **34** (2007) 2307.
- [27] N. Schul and K. Piotrkowski, Nucl. Phys. Proc. Suppl. **179-180** (2008) 289.
- [28] B. Alessandro *et al.* [ALICE Collaboration], J. Phys. G **32** (2006) 1295; J. Nystrand [ALICE Collaboration], Nucl. Phys. Proc. Suppl. **179-180** (2008) 156.